ELSEVIER

Chemical Geology 227 (2006) 258–273

CHEMICAL GEOLOGY
INCLUDING
ISOTOPE GEOSCIENCE

www.elsevier.com/locate/chemgeo

A $^{40}Ar/^{39}Ar$ and U/Pb isotopic study of the Ilímaussaq complex, South Greenland: Implications for the ^{40}K decay constant and for the duration of magmatic activity in a peralkaline complex

Thomas V. Krumrei [a], Igor M. Villa [b,c,*], Michael A.W. Marks [a], Gregor Markl [a]

[a] *Eberhard Karls Universität Tübingen, Institut für Geowissenschaften, Wilhelmstr. 56, D-72074 Tübingen, Germany*
[b] *University of Bern, Institut für Geologie, Baltzerstrasse 1, 3012 Bern, Switzerland*
[c] *Università di Milano Bicocca, Dipartimento di Scienze Geologiche e Geotecnologie, 20126 Milano, Italy*

Received 18 October 2004; received in revised form 7 October 2005; accepted 11 October 2005

Abstract

Magmatism in the Gardar Province, South Greenland, is related to two main rifting events at 1280 Ma and 1180 to 1140 Ma. Little is known about the duration of the magmatic activity in a specific complex. The Ilímaussaq intrusion belongs to the second period of rifting and comprises an extraordinary diversity of granitic and syenitic rock types, which intruded and fractionated in three successive magmatic events. As the intrusion contains some of the most evolved, incompatible element-rich rocks on Earth, it was chosen for a detailed geochronological study to quantify the duration of melt production, intrusion, fractionation and cooling. Amphiboles, which are abundant in all rock types, including pegmatites and late magmatic veins, were dated using the $^{40}Ar/^{39}Ar$ technique. Since the solidus temperature of the most evolved melts is below the closure temperature of amphibole, and no later heating event occurred, the $^{40}Ar/^{39}Ar$ ages reflect the magmatic crystallisation and can be used to determine the duration of igneous differentiation. The $^{40}Ar/^{39}Ar$ plateau ages range between 1142.6 ± 2.2 Ma and 1152.3 ± 3.7 Ma using the Steiger and Jäger [Steiger, R.H. and Jäger, E., (1977). Subcommision on Geochronology: convention on the use of decay constants in geo- and cosmochronology. Earth Planet. Sci. Lett. 36, 359–362.] ^{40}K decay constant. These ages are younger than an U–Pb age of 1160 ± 5 Ma on baddeleyite from the first magma batch. Our results indicate that the ^{40}K decay constant of Steiger and Jäger may be too high; a lambda similar to that proposed by Kwon et al. [Kwon, J., Min, K., Bickel, P. and Renne, P.R., (2002). Statistical methods for jointly estimating decay constant of ^{40}K and age of a dating standard. Math. Geol. 34, 457–474.] is required to make the $^{40}Ar/^{39}Ar$ match the U–Pb age.

Keywords: Peralkaline; $^{40}Ar/^{39}Ar$ ages; ^{40}K decay constant; Geochronology; Ilímaussaq

1. Introduction

The Mesoproterozoic Ilímaussaq igneous complex is one of ten alkaline intrusive bodies in the Gardar Province, South Greenland. Since the first detailed description by Ussing (1912) who introduced the term agpaitic nepheline syenites for peralkaline rocks containing complex Zr–Ti silicates like eudialyte and rinkite, numerous papers dealing with the Ilímaussaq complex have been published (e.g. Sørensen and Larsen, 1987; Rose-Hansen et al., 2001; Markl et al., 2001a,b; Marks and Markl, 2001). The detailed chronology of the complex, however, and the time needed

* Corresponding author. University of Bern, Institut für Geologie, Baltzerstrasse 1, 3012 Bern, Switzerland. Tel.: +41 31 631 87 77; fax: +41 31 631 49 88.
E-mail address: igor@geo.unibe.ch (I.M. Villa).

0009-2541/$ - see front matter © 2005 Elsevier B.V. All rights reserved.
doi:10.1016/j.chemgeo.2005.10.004

to evolve to the most fractionated rocks, are still a matter of debate. Investigations from other alkaline provinces (e.g. Namibia, East African rift system) suggest that the formation of evolved and non-evolved rocks may be contemporaneous (Heaman and Machado, 1992; Harris et al., 1999; Mingram et al., 2000; Schmitt et al., 2000). Geochronological studies of the alkaline rocks from the Kola Peninsula (Kramm et al., 1993; Kramm and Kogarko, 1994; Arzamastsev et al., 2000) do not have the necessary resolution to judge the formation history of single complexes, but it appears that there is no hiatus in the development within the single complexes. Evidence from peralkaline rocks (e.g. Azores, Kenya) indicate very short timescales of fractionation, i.e. only tens of thousands of years (Widom et al., 1992; Bourdon et al., 1994; Rogers et al., 2004). In non-peralkaline magmatic provinces, the differentiation from andesitic to rhyolitic rocks needs a few hundred thousand years depending on the Si-content of the melts (Christensen and DePaolo, 1993; Reid et al., 1997; Hawkesworth et al., 2000; Reagan et al., 2003).

The Ilímaussaq complex is specifically suited for studying the duration of processes of magma evolution and the quantification of such processes because the complex is made up of three distinct magma batches that are successively more evolved and which include some of the most fractionated rocks on Earth. Additionally, the rocks are well exposed, easy to distinguish in the field and their petrography, petrology and geochemistry are very well known (e.g. Ferguson, 1964; Sørensen and Larsen, 1987; Bailey et al., 2001; Markl et al., 2001a; Marks et al., 2004). The intrusion level was shallow and no metamorphic overprint is recorded since the time of intrusion (Upton et al., 2003).

The Ilímaussaq complex is also suited for a comparison and examination of dating methods using isotopic systems because it has been dated by different independent methods. Blaxland et al. (1976) presented Rb–Sr data, from which they calculated a whole rock isochron

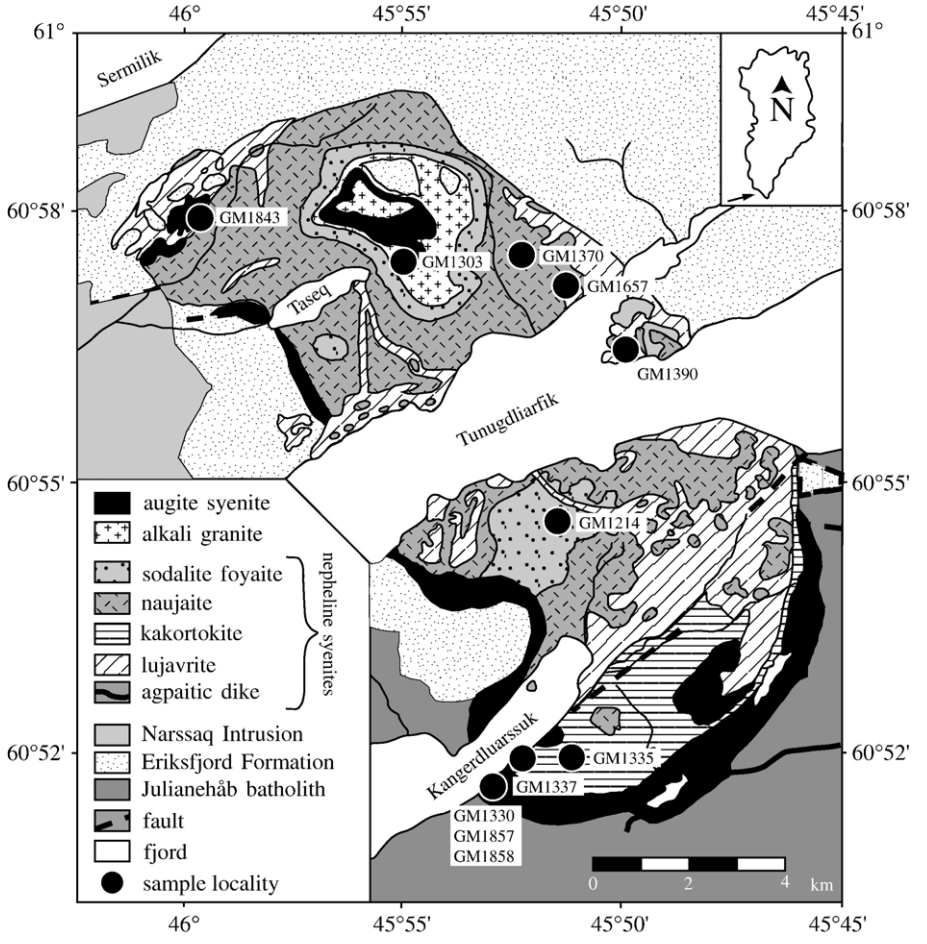

Fig. 1. Geological map of Ilímaussaq with sample localities, modified after Ferguson (1964).

of 1168 ± 21 Ma (MSWD = 3.6). Paslick et al. (1993) obtained 1130 ± 50 Ma (MSWD = 0.08) from a Sm–Nd whole rock–mineral isochron whereas Marks et al. (2004) calculated 1160 ± 30 Ma (MSWD = 3.7) from their Sm–Nd data. More precise results are given by a U–Pb radiometric date of the second magma pulse (alkali granite, 1166 ± 9 Ma, Heaman and Upton, cited in Upton et al., 2003) and by a Rb–Sr age of a late agpaitic rock of 1160.1 ± 2.3 Ma (Waight et al., 2002). In this paper we present a detailed dating study including $^{40}Ar/^{39}Ar$ ages of amphiboles from the major rock types and late stage pegmatites and a new U–Pb age of baddeleyite from the earliest magma pulse (augite syenite).

2. Geology

Magmatism in the Gardar Province, South Greenland, is closely related to rifting between 1350 and 1140 Ma. Based on U–Pb chronology, two main periods of magmatic activity around 1280 Ma and between 1180 and 1140 Ma, respectively, can be separated (Upton et al., 2003). During these time spans, several alkaline to peralkaline plutonic complexes and a large number of dykes with variable compositions intruded the Ketilidian (1.7–1.8 Ga) granitic basement rocks (Julianehåb granite). The Ilímaussaq intrusion belongs to the second period (Blaxland et al., 1976) and consists of alkaline, peralkaline and agpaitic (i.e. (Na + K)/Al > 1.2, Ussing, 1912) rocks. Controlled by early fault systems (Sørensen, 1966), the complex intruded at the contact between the Julianehåb granite and the late-Gardar Eriksfjord formation that consists mainly of basalts and sandstones (Poulsen, 1964).

Three pulses of magma intruded successively to 3–4 km depth (Larsen and Sørensen, 1987). The first one produced a silica-saturated to slightly under-saturated augite syenite, which is now found as the outer shell of the intrusion. Subsequently, a sheet of a peralkaline granite (in the literature on Ilímaussaq called alkali granite) intruded the augite syenite. According to Marks et al. (2004), this represents a more evolved and crustally contaminated equivalent of the augite syenite that possibly assimilated 10% to 15% of siliceous Archeaen lower crustal rocks. In a third stage, various agpaitic nepheline syenites (sodalite foyaite, naujaite, kakortokite and lujavrite) were formed by low-pressure in situ fractionation of a broadly phonolitic melt. They contain nepheline, eudialyte, sodalite, alkali feldspar, aegirine and arfvedsonite in various proportions as well as rare minerals like rinkite, aenigmatite, neptunite and others. These agpaites make up the major part of the complex (Fig. 1). The sodalite foyaite and the naujaite are cumulates formed at the roof of the magma chamber by flotation of minerals less dense than the melt, whereas the strongly layered kakortokites are interpreted as cumulates on the bottom of the magma chamber. The lujavrites form intrusive

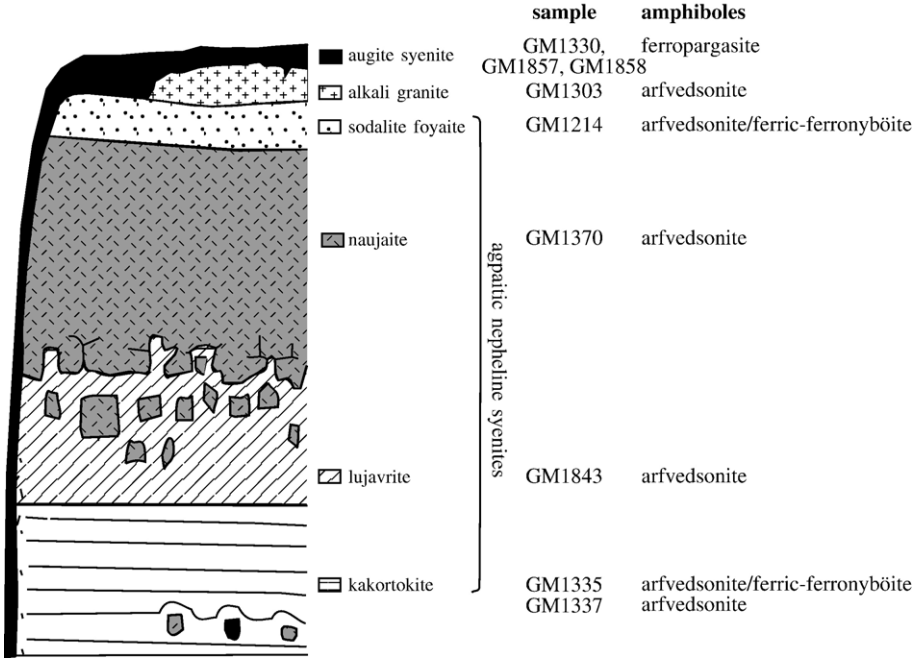

Fig. 2. Schematic profile of the Ilímaussaq complex summarising the geology, the stratigraphic position of the samples and amphibole types.

contacts to the other rocks and are interpreted as the residual melts between the roof and bottom cumulates intruding along fractures into the earlier solidified cumulates. Numerous pegmatites and late-magmatic to hydrothermal veins occur all over the intrusion.

We are aware of the problems in using non-recommended rock names. However, the alternative of using only recommended nomenclature would mean that all rocks would be lumped together as "nepheline syenite" despite their striking differences. Since the names for these exotic rocks are well established in the literature, we use them to discriminate our samples and make possible their attribution to the different subunits of the Ilímaussaq complex. Fig. 2 provides a survey of rock types, their stratigraphic position, the position of the samples and types of amphiboles.

Several publications mainly dealing with the isotopic composition of the rocks show that the different magma batches, starting with the augite syenite and ending with the lujavrites, originated from a single source (Nielsen and Steenfelt, 1979; Larsen and Sørensen, 1987; Stevenson et al., 1997; Marks et al., 2004). The extreme fractionation trend found in the Ilímaussaq complex appears to be governed by low water activity, low SiO_2 activity and low oxygen fugacity in the parental melt (Larsen, 1976, 1977, 1981; Markl et al., 2001a,b; Marks and Markl, 2001).

3. Petrography and mineral chemistry

The petrography of the Ilímaussaq rocks is reported in many publications (e.g. Ferguson, 1964; Sørensen, 2001). Amphibole occurs in all rock types of the complex. Most of the samples used in this study are described in Marks et al. (2004) with a focus on amphibole and aegirine textures. Chemical analyses of the amphiboles and pictures of amphibole textures are also presented therein. Microprobe analyses of amphiboles from the three samples GM1335, GM1390 and GM1657 not published in Marks et al. (2004) are given in Table 1. The early augite syenite contains Ca-rich amphiboles (ferro-edenite, ferro-pargasite). In this rock, amphibole occurs in two generations, as a magmatic phase and as later overgrowths on olivine. The latter

Table 1
Selected microprobe analyses of amphibole from samples GM1335, GM1390 and GM1657 not published in Marks et al. (2004)

Sample rock type	GM1335 kakortokite (red)		GM1390 agpaitic pegmatite		GM1657 agpaitic pegmatite	
SiO_2	45.48	43.45	47.74	49.6	47.61	47.81
TiO_2	0.75	0.69	0.74	0.64	0.57	0.42
Al_2O_3	1.23	2.59	0.93	0.89	2.41	2.01
FeO	34.67	35.15	32.75	32.9	34.61	34.25
MnO	0.93	0.79	1.12	1.24	0.44	0.41
MgO	0.53	0.86	0.10	0.19	0.19	0.11
CaO	0.69	2.67	0.29	0.22	1.43	1.56
Na_2O	8.10	7.61	8.41	8.30	8.10	8.56
K_2O	2.60	1.62	2.57	3.03	1.80	1.61
ZrO_2	0.08	0.43	b.d.	0.07	n.a.	0.34
Cl	n.a.	n.a.	b.d.	b.d.	b.d.	0.01
F	0.84	0.71	0.12	b.d.	0.91	0.84
Total	95.90	96.57	94.77	97.08	98.07	97.93
Formulae based on 16 cations and 23 oxygens						
Si	7.435	7.075	7.812	7.920	7.617	7.639
Al	0.237	0.497	0.179	0.167	0.454	0.379
Ti	0.092	0.085	0.091	0.077	0.069	0.050
Fe^{3+}	1.805	1.855	1.219	1.015	1.055	1.169
Mg	0.129	0.209	0.024	0.045	0.045	0.026
Fe^{2+}	2.936	2.932	3.263	3.378	3.576	3.407
Mn	0.129	0.109	0.155	0.168	0.060	0.055
Ca	0.121	0.466	0.051	0.038	0.245	0.267
Na	2.568	2.403	2.668	2.570	2.512	2.652
K	0.542	0.337	0.537	0.617	0.367	0.328
Zr	0.006	0.034		0.005		0.026
Cl						0.003
F	0.434	0.366	0.062		0.460	0.424
Sum	16.000	16.000	16.000	16.000	16.000	16.000

n.a. = not analysed, b.d. = below detection limit.

was excluded during hand picking. Amphibole in the alkali granite is an early magmatic phase. In the more evolved rocks, amphiboles are also of clearly magmatic origin. In some samples they form euhedral crystals (black kakortokite, lujavrite), in others they occur interstitially (sodalite foyaite, naujaite, red kakortokite). The only sample not described texturally in Marks et al. (2004), the pegmatitic sample GM1657, is similar to sample GM1390 but the size of the crystals is still larger, up to half a meter. All amphiboles from the agpaitic rocks show enrichments in Na (nyböite, arfvedsonite) and contain elevated amounts of Li (up to 2500 ppm), Zn (5600 ppm) and Zr (5000 ppm). In the augite syenite, the lujavrite and in the naujaite, the amphiboles show a chemical zonation. Since all amphiboles contain at least 1.5% K_2O, they are well suited for dating with the $^{40}Ar/^{39}Ar$ technique. Numerous studies showed that the Ilímaussaq intrusion as well as the whole Gardar Province did not experience any metamorphic overprint after the end of magmatic activity (Markl, 2001; Markl et al., 2001b; Sørensen, 2001; Upton et al., 2003).

Baddeleyite is an early phase in the augite syenite as indicated by the occurrence as inclusions in olivine, clinopyroxene, feldspar and Fe–Ti-oxide minerals. The crystals are euhedral but in most cases smaller than 0.5 mm. A BSE image of a baddeleyite texture can be found in Marks and Markl (2001). The textures show that baddeleyite is clearly a primary phase crystallised from the augite syenite magma. Neither BSE images nor CL images indicate zonations or other chemical variations within the baddeleyite crystals. Inheritance from the country rocks of the Ilímaussaq intrusion can be excluded because of the lack of baddeleyite in these rocks. Two samples of the augite syenite were chosen for the extraction of baddeleyite (GM1857 and GM1858). GM1857 is a fine-grained variety taken close to the contact to the country rocks. The locality of the coarse-grained augite syenite GM1858 is close to the inner contact to the agpaites. Both sample localities have a distance to the respective contact of approximately 20 m.

4. Analytical techniques

4.1. $^{40}Ar/^{39}Ar$ technique

The rock samples were crushed and sieved. Amphiboles were enriched by gravimetric and magnetic means and finally handpicked from the 250–180 μm grain size fraction to ensure visual purity. The samples were irradiated at the McMaster reactor, Ontario, Canada including the MMhb standard (McClure Mountain hornblende) with an age of 523.1 Ma (Renne et al., 1998). The analyses of the Ar isotopes were performed at the University of Bern and the analytical procedure of stepwise heating is described in Villa et al. (2000).

4.2. U–Pb technique

Baddeleyite was concentrated by gravimetric means and finally handpicked. It was analysed using conventional U–Pb analytical techniques. Separated and washed grains were spiked with a mixed $^{205}Pb/^{235}U$ tracer and digested in 22 N HF at 200 °C for one week in a Parr bomb. Chemical separation of U and Pb was made using ion exchange techniques similar to those described by Chen et al. (2000) for zircon analyses. Uranium and lead were isotopically analysed on a Finnigan MAT 262 mass spectrometer at the University of Tübingen. Initial common Pb remaining after correction for tracer and blank was corrected using values from the Stacey and Kramers (1975) model. U–Pb data were calculated and plotted with software from Ludwig (1988, 2003).

5. Results

5.1. $^{40}Ar/^{39}Ar$ dating

Amphibole releases its Ar by a dehydration reaction to pyroxene and feldspar and by a melting reaction, respectively (Wartho et al., 1991; Lee, 1993). Therefore, the release pattern of an unzoned amphibole displays two maxima with the first maximum being dominant. The temperature of these reactions depends on the chemical composition (Villa et al., 2000). Ca- and Mg-rich amphiboles (magnesiohastingsite, actinolite) degas at higher temperatures than Na-rich amphiboles (riebeckite). Our Na-dominated amphiboles (mainly arfvedsonite) have their first maximum of degassing at temperatures between 680 and 800 °C, which extends the range of degassing rates of various amphibole compositions given in Fig. 3a in Villa et al. (2000) to lower temperatures. In contrast, sample GM1330 from the augite shows a first degassing peak at 980 °C in accordance with its Ca-dominated composition. One sample (GM1214, the sodalite foyaite) degasses continuously over a wide temperature range between 700 and 1200 °C (see Fig. A1 in the Electronic Supplement). In contrast to the chemical zonation of some of the amphiboles, systematic variations in Ca/K or Cl/K ratios during stepwise heating were found only in sample GM1303 where the age correlates with Cl/K. This means that zones of

Table 2
Isotopic composition of the released Ar

Step	T (°C)	$^{40}Ar_{tot}$	^{39}Ar	^{38}Ar	^{37}Ar	^{36}Ar	Age ± 1σ
GM1330	10.0 mg; $J=3.825*10^{-3}$; $K_2O=1.60$; CaO=9.61; plateau age=1150.2 ± 4.2; MSWD=5.4% ^{39}Ar in Ar plateau=50.7						
1	586	233.25 ± 0.00	0.962 ± 0.017	b.d.	1.761 ± 0.072	0.282 ± 0.010	845.2 ± 18.0
2	656	519.57 ± 0.01	2.021 ± 0.019	0.145 ± 0.017	1.751 ± 0.055	0.459 ± 0.016	985.8 ± 12.0
3	786	1384.27 ± 0.16	5.645 ± 0.017	0.245 ± 0.013	1.505 ± 0.031	0.337 ± 0.017	1130.0 ± 4.2
4*	913	2376.65 ± 0.28	9.883 ± 0.017	1.056 ± 0.004	9.977 ± 0.089	0.292 ± 0.020	1145.9 ± 2.6
5*	975	17,761.20 ± 2.60	75.786 ± 0.072	22.574 ± 0.042	212.075 ± 0.605	0.397 ± 0.019	1151.3 ± 0.9
6*	997	13,495.80 ± 2.40	57.688 ± 0.056	17.428 ± 0.038	168.227 ± 0.489	0.222 ± 0.011	1151.4 ± 0.9
7*	1014	5443.33 ± 0.69	23.250 ± 0.030	6.921 ± 0.027	67.715 ± 0.209	0.231 ± 0.022	1145.4 ± 1.5
8	1028	6161.59 ± 1.00	26.047 ± 0.042	7.849 ± 0.021	77.250 ± 0.247	0.522 ± 0.012	1143.5 ± 1.5
9	1064	2428.27 ± 0.16	10.324 ± 0.019	2.949 ± 0.031	32.018 ± 0.118	0.150 ± 0.013	1144.6 ± 2.0
10	1085	913.03 ± 0.08	3.646 ± 0.033	1.131 ± 0.023	14.501 ± 0.153	0.248 ± 0.015	1143.2 ± 8.9
11	1118	1856.12 ± 0.23	7.863 ± 0.030	2.397 ± 0.037	32.619 ± 0.169	0.242 ± 0.021	1130.9 ± 4.3
12	1154	1415.39 ± 0.17	5.996 ± 0.047	1.749 ± 0.026	34.893 ± 0.299	0.156 ± 0.016	1137.5 ± 7.2
13	1203	1194.36 ± 0.24	5.044 ± 0.017	1.508 ± 0.015	52.465 ± 0.230	0.188 ± 0.020	1131.8 ± 4.9
14	1449	22,106.40 ± 1.20	94.585 ± 0.092	28.199 ± 0.052	368.223 ± 1.038	0.362 ± 0.018	1151.4 ± 0.8
GM1214	9.7 mg; $J=3.830*10^{-3}$; $K_2O=1.86$; CaO=2.60; plateau age=1142.6 ± 2.2; MSWD=2.2% ^{39}Ar in plateau=43.8						
1	584	225.59 ± 0.25	1.052 ± 0.015	0.250 ± 0.011	1.029 ± 0.074	0.287 ± 0.012	747.8 ± 19.0
2	648	1305.89 ± 0.00	5.877 ± 0.024	0.153 ± 0.023	2.036 ± 0.035	0.455 ± 0.019	1023.6 ± 4.8
3	697	8363.73 ± 0.79	36.162 ± 0.042	0.706 ± 0.021	15.381 ± 0.070	0.541 ± 0.011	1128.5 ± 1.0
4	742	11,849.07 ± 0.78	50.836 ± 0.052	1.200 ± 0.011	28.489 ± 0.125	0.515 ± 0.019	1140.6 ± 0.9
5*	781	13,305.77 ± 1.13	57.156 ± 0.056	1.212 ± 0.019	39.686 ± 0.123	0.391 ± 0.008	1143.2 ± 0.9
6*	819	11,726.60 ± 0.98	50.468 ± 0.053	1.183 ± 0.019	48.059 ± 0.149	0.288 ± 0.024	1143.0 ± 1.0
7*	877	14,212.78 ± 1.13	61.066 ± 0.059	1.123 ± 0.023	37.600 ± 0.119	0.383 ± 0.013	1143.5 ± 0.9
8	932	14,012.78 ± 1.13	60.014 ± 0.057	1.301 ± 0.022	44.087 ± 0.132	0.232 ± 0.012	1149.0 ± 0.8
9	1039	13,811.13 ± 0.43	59.298 ± 0.058	1.581 ± 0.033	73.094 ± 0.216	0.436 ± 0.016	1143.5 ± 0.9
10	1454	798.11 ± 0.14	2.975 ± 0.011	0.122 ± 0.008	3.691 ± 0.039	0.463 ± 0.009	1112.4 ± 4.6
GM1303	9.5 mg; $J=3.861*10^{-3}$; $K_2O=1.51$; CaO=1.06; plateau age=1152.3 ± 3.7; MSWD=5.1% ^{39}Ar in plateau=71.2						
1	586	323.13 ± 0.56	2.013 ± 0.031	0.272 ± 0.031	1.682 ± 0.052	0.227 ± 0.019	720.9 ± 16.0
2	634	662.70 ± 0.06	3.124 ± 0.025	0.337 ± 0.022	2.692 ± 0.066	0.331 ± 0.017	955.4 ± 9.0
3	713	10,253.36 ± 0.80	44.032 ± 0.052	3.778 ± 0.028	15.555 ± 0.108	0.494 ± 0.015	1145.0 ± 1.1
4*	792	25,265.16 ± 0.75	107.877 ± 0.102	9.666 ± 0.039	36.907 ± 0.119	0.858 ± 0.021	1153.5 ± 0.8
5*	824	4773.71 ± 0.22	20.290 ± 0.028	1.823 ± 0.023	7.626 ± 0.095	0.265 ± 0.032	1151.9 ± 2.1
6*	866	10,379.20 ± 0.27	44.479 ± 0.043	3.790 ± 0.031	14.144 ± 0.096	0.390 ± 0.013	1149.4 ± 0.9
7*	912	11,856.95 ± 0.59	50.664 ± 0.049	4.697 ± 0.032	19.383 ± 0.096	0.347 ± 0.032	1154.1 ± 1.1
8	955	4854.21 ± 0.22	20.615 ± 0.034	1.968 ± 0.015	10.037 ± 0.082	0.196 ± 0.017	1156.5 ± 1.6
9	994	2718.83 ± 0.21	11.763 ± 0.025	0.893 ± 0.018	5.925 ± 0.076	0.216 ± 0.017	1130.8 ± 2.4
10	1034	1153.09 ± 0.20	5.019 ± 0.045	0.427 ± 0.033	2.941 ± 0.065	0.223 ± 0.015	1096.7 ± 8.1
11	1450	883.14 ± 0.14	3.672 ± 0.021	0.229 ± 0.041	2.330 ± 0.079	0.440 ± 0.021	1052.4 ± 8.0
GM1335	9.8 mg; $J=3.865*10^{-3}$; $K_2O=1.69$; CaO=1.43; plateau age=1152.3 ± 1.8; MSWD=2.6% ^{39}Ar in plateau=81.5						
1	583	678.71 ± 0.41	3.595 ± 0.034	0.402 ± 0.032	2.107 ± 0.077	0.468 ± 0.017	826.7 ± 8.8
2	680	7434.04 ± 0.43	32.124 ± 0.042	1.389 ± 0.024	12.019 ± 0.111	0.393 ± 0.023	1139.4 ± 1.4
3*	724	22,421.84 ± 1.73	95.707 ± 0.088	2.855 ± 0.029	39.386 ± 0.134	0.695 ± 0.018	1155.4 ± 0.8
4*	762	7795.94 ± 0.28	33.303 ± 0.039	0.799 ± 0.020	15.096 ± 0.067	0.254 ± 0.022	1154.3 ± 1.2
5*	814	4893.16 ± 0.19	20.961 ± 0.029	0.558 ± 0.021	9.993 ± 0.064	0.154 ± 0.030	1152.3 ± 1.9
6*	846	7855.78 ± 0.18	33.715 ± 0.038	1.011 ± 0.030	14.411 ± 0.071	0.257 ± 0.027	1150.3 ± 1.3
7*	885	13,539.29 ± 0.31	58.070 ± 0.060	1.683 ± 0.018	25.632 ± 0.104	0.352 ± 0.017	1152.6 ± 0.9
8*	926	10,697.55 ± 0.47	45.656 ± 0.048	1.930 ± 0.028	25.636 ± 0.082	0.415 ± 0.011	1153.6 ± 0.9
9	981	3975.28 ± 0.23	17.071 ± 0.029	0.861 ± 0.024	10.464 ± 0.055	0.223 ± 0.019	1144.0 ± 1.9
10	1031	1239.02 ± 0.10	5.305 ± 0.013	0.137 ± 0.018	2.852 ± 0.045	0.146 ± 0.015	1130.5 ± 3.8
11	1451	1623.61 ± 0.29	6.830 ± 0.028	0.318 ± 0.022	3.543 ± 0.079	0.268 ± 0.016	1133.2 ± 4.3
GM1337	8.6 mg; $J=3.820*10^{-3}$; $K_2O=1.92$; CaO=1.56; total gas age=1134.2						
1	584	323.34 ± 0.56	1.760 ± 0.049	0.922 ± 0.029	1.282 ± 0.077	0.414 ± 0.012	653.5 ± 18.0
2	651	779.08 ± 0.20	3.029 ± 0.026	1.583 ± 0.020	2.052 ± 0.059	0.810 ± 0.020	936.8 ± 10.0

(continued on next page)

Table 2 (*continued*)

Step	T (°C)	$^{40}Ar_{tot}$	^{39}Ar	^{38}Ar	^{37}Ar	^{36}Ar	Age ± 1σ
GM1337	8.6 mg; $J=3.820*10^{-3}$; $K_2O=1.92$; CaO=1.56; total gas age=1134.2						
3	681	4491.93 ± 0.47	19.109 ± 0.028	2.101 ± 0.027	7.366 ± 0.083	0.760 ± 0.016	1112.9 ± 1.6
4	712	7064.73 ± 1.08	29.748 ± 0.035	1.723 ± 0.019	11.576 ± 0.094	0.763 ± 0.016	1137.3 ± 1.2
5	743	10,439.24 ± 1.86	44.560 ± 0.058	1.926 ± 0.023	17.177 ± 0.107	0.584 ± 0.024	1139.1 ± 1.3
6	765	11,425.45 ± 3.02	48.672 ± 0.051	1.589 ± 0.027	19.352 ± 0.083	0.652 ± 0.010	1140.5 ± 1.0
7	790	7973.21 ± 0.60	33.937 ± 0.037	0.989 ± 0.031	14.027 ± 0.063	0.439 ± 0.015	1141.8 ± 1.1
8	850	8397.65 ± 0.67	35.991 ± 0.048	1.369 ± 0.024	16.475 ± 0.070	0.466 ± 0.016	1135.8 ± 1.2
9	897	15,511.98 ± 0.92	66.343 ± 0.069	2.604 ± 0.045	27.967 ± 0.129	0.497 ± 0.027	1143.5 ± 1.0
10	938	13,827.44 ± 0.57	59.140 ± 0.059	2.176 ± 0.029	26.621 ± 0.089	0.633 ± 0.022	1140.0 ± 0.9
11	988	8275.45 ± 0.35	35.674 ± 0.041	1.533 ± 0.013	21.704 ± 0.075	0.427 ± 0.015	1132.0 ± 1.1
12	1036	3331.77 ± 0.34	14.329 ± 0.023	0.573 ± 0.017	7.938 ± 0.064	0.332 ± 0.021	1121.7 ± 2.1
13	1458	777.29 ± 0.23	2.726 ± 0.026	0.098 ± 0.016	1.130 ± 0.069	0.556 ± 0.021	1118.9 ± 11.0
GM1370	9.9 mg; $J=3.845*10^{-3}$; $K_2O=2.09$; CaO=2.61; total gas age=1165.0						
1	583	767.07 ± 0.09	3.438 ± 0.017	1.599 ± 0.014	1.852 ± 0.060	0.426 ± 0.017	975.7 ± 7.1
2	652	8653.19 ± 1.01	37.426 ± 0.042	3.840 ± 0.015	21.236 ± 0.107	0.716 ± 0.008	1127.1 ± 1.0
3	683	28,966.67 ± 2.93	122.225 ± 0.111	6.069 ± 0.022	66.361 ± 0.195	1.093 ± 0.014	1159.5 ± 0.8
4	711	9420.75 ± 0.31	39.798 ± 0.042	1.944 ± 0.016	27.298 ± 0.090	0.530 ± 0.018	1153.8 ± 1.0
5	738	7597.06 ± 0.32	32.385 ± 0.035	1.716 ± 0.020	25.967 ± 0.107	0.270 ± 0.011	1151.5 ± 1.0
6	785	9100.86 ± 0.22	38.544 ± 0.038	2.376 ± 0.017	35.632 ± 0.108	0.251 ± 0.021	1159.2 ± 1.0
7	837	8206.00 ± 0.31	33.885 ± 0.037	2.548 ± 0.020	25.056 ± 0.080	0.470 ± 0.015	1173.1 ± 1.0
8	883	12,325.25 ± 0.64	49.706 ± 0.048	3.475 ± 0.012	27.327 ± 0.092	0.573 ± 0.016	1196.3 ± 0.9
9	928	10,484.24 ± 0.57	41.794 ± 0.044	3.415 ± 0.023	31.223 ± 0.117	0.634 ± 0.017	1203.0 ± 1.0
10	979	5486.80 ± 0.27	22.314 ± 0.023	2.028 ± 0.021	22.071 ± 0.072	0.334 ± 0.017	1185.6 ± 1.2
11	1030	1532.72 ± 0.17	6.304 ± 0.023	0.636 ± 0.017	5.340 ± 0.066	0.234 ± 0.015	1151.8 ± 4.1
12	1449	1205.88 ± 0.00	4.778 ± 0.023	0.297 ± 0.015	3.700 ± 0.055	0.311 ± 0.016	1155.3 ± 5.6
GM1390	10.4 mg; $J=3.840*10^{-3}$; $K_2O=2.85$; CaO=0.29; total gas age=1148.6						
1	586	400.06 ± 0.16	1.724 ± 0.017	0.104 ± 0.016	1.037 ± 0.021	0.532 ± 0.017	780.1 ± 14.0
2	652	6583.85 ± 0.85	27.943 ± 0.042	0.612 ± 0.044	1.886 ± 0.063	0.817 ± 0.028	1130.8 ± 1.7
3	698	31,546.73 ± 0.84	134.986 ± 0.125	2.153 ± 0.022	6.897 ± 0.064	0.941 ± 0.016	1148.0 ± 0.8
4	749	50,780.50 ± 0.30	216.015 ± 0.221	2.566 ± 0.007	11.349 ± 0.078	0.856 ± 0.032	1156.3 ± 0.9
5	791	11,547.40 ± 1.63	48.899 ± 0.053	0.925 ± 0.026	2.303 ± 0.032	0.950 ± 0.019	1143.5 ± 1.0
6	844	11,246.92 ± 1.54	47.896 ± 0.048	0.932 ± 0.009	2.619 ± 0.038	0.624 ± 0.020	1145.5 ± 1.0
7	892	7781.25 ± 1.15	32.952 ± 0.037	0.547 ± 0.020	2.127 ± 0.040	0.564 ± 0.020	1145.9 ± 1.2
8	933	8630.54 ± 0.24	36.655 ± 0.040	0.449 ± 0.022	2.096 ± 0.026	0.332 ± 0.019	1152.1 ± 1.1
9	1036	9027.99 ± 2.31	38.628 ± 0.046	0.630 ± 0.019	2.084 ± 0.035	0.429 ± 0.021	1143.5 ± 1.2
10	1458	637.22 ± 0.09	1.993 ± 0.031	b.d.	b.d.	0.584 ± 0.015	1153.4 ± 16.0
GM1657	9.4 mg; $J=3.835*10^{-3}$; $K_2O=1.92$; CaO=1.30; plateau age=1145.5 ± 1.7; MSWD=2.0% ^{39}Ar in plateau=59.7						
1	586	572.99 ± 0.01	2.291 ± 0.021	0.213 ± 0.026	1.526 ± 0.065	0.433 ± 0.017	1005.1 ± 11.0
2	651	4720.64 ± 0.46	20.017 ± 0.026	0.605 ± 0.019	6.992 ± 0.050	0.372 ± 0.017	1142.4 ± 1.4
3	696	18,728.51 ± 1.60	80.208 ± 0.073	1.396 ± 0.022	28.455 ± 0.096	0.665 ± 0.023	1145.0 ± 0.8
4	738	11,332.45 ± 1.60	48.798 ± 0.056	0.888 ± 0.011	18.436 ± 0.105	0.385 ± 0.014	1140.8 ± 1.0
5*	765	5220.19 ± 0.30	22.434 ± 0.032	0.259 ± 0.016	8.319 ± 0.087	0.142 ± 0.014	1144.2 ± 1.4
6*	791	4326.51 ± 1.06	18.531 ± 0.028	0.193 ± 0.015	6.717 ± 0.057	0.184 ± 0.008	1143.1 ± 1.4
7*	828	8297.00 ± 0.78	35.792 ± 0.040	0.787 ± 0.011	12.859 ± 0.054	0.097 ± 0.011	1144.9 ± 1.0
8*	863	16,594.26 ± 0.65	71.361 ± 0.073	1.157 ± 0.022	25.949 ± 0.093	0.199 ± 0.024	1147.4 ± 1.0
9*	909	17,099.47 ± 1.49	73.646 ± 0.080	1.287 ± 0.024	27.803 ± 0.103	0.262 ± 0.020	1145.3 ± 1.0
10*	952	3566.13 ± 0.67	14.989 ± 0.022	0.106 ± 0.015	5.886 ± 0.050	0.307 ± 0.015	1148.0 ± 1.7
11	1031	1092.50 ± 0.16	4.546 ± 0.018	0.163 ± 0.024	1.946 ± 0.048	0.237 ± 0.011	1122.3 ± 4.3
12	1446	1018.55 ± 0.38	4.139 ± 0.015	0.159 ± 0.017	1.303 ± 0.033	0.365 ± 0.011	1104.2 ± 4.1
GM1843	10.0 mg; $J=3.853*10^{-3}$; $K_2O=3.24$; CaO=0.19; total gas age=1138.7						
1	586	1197.25 ± 0.13	5.949 ± 0.012	0.155 ± 0.022	1.157 ± 0.042	0.482 ± 0.015	939.4 ± 3.3
2	652	27,309.30 ± 0.52	117.361 ± 0.110	1.554 ± 0.029	3.581 ± 0.036	0.863 ± 0.019	1146.7 ± 0.8
3	674	43,977.65 ± 0.38	191.426 ± 0.035	2.939 ± 0.029	6.787 ± 0.055	0.680 ± 0.015	1141.1 ± 1.2
4	697	20,154.40 ± 1.70	87.697 ± 0.083	1.308 ± 0.026	2.620 ± 0.070	0.260 ± 0.019	1140.9 ± 0.8
5	727	4935.66 ± 0.33	21.985 ± 0.030	0.154 ± 0.030	0.585 ± 0.052	0.212 ± 0.018	1113.8 ± 1.4

Table 2 (*continued*)

Step	T (°C)	$^{40}Ar_{tot}$	^{39}Ar	^{38}Ar	^{37}Ar	^{36}Ar	Age ± 1σ
GM1843	10.0 mg; $J=3.853*10^{-3}$; $K_2O=3.24$; CaO=0.19; total gas age=1138.7						
6	768	8925.51 ± 1.30	39.166 ± 0.044	0.483 ± 0.016	1.120 ± 0.069	0.099 ± 0.015	1134.3 ± 1.0
7	818	20,532.60 ± 0.77	89.351 ± 0.083	1.158 ± 0.029	2.954 ± 0.094	0.160 ± 0.018	1142.1 ± 0.8
8	866	21,807.70 ± 0.98	94.979 ± 0.092	1.204 ± 0.024	3.364 ± 0.071	0.000 ± 0.014	1143.8 ± 0.8
9	911	3937.32 ± 0.20	17.485 ± 0.025	0.379 ± 0.023	0.600 ± 0.049	0.120 ± 0.015	1119.4 ± 1.5
10	952	1744.40 ± 0.17	7.515 ± 0.021	0.067 ± 0.020	0.259 ± 0.049	0.030 ± 0.011	1148.3 ± 2.9
11	1033	1169.91 ± 0.20	4.833 ± 0.019	0.049 ± 0.028	0.366 ± 0.077	0.054 ± 0.013	1176.8 ± 4.5
12	1454	730.49 ± 0.01	3.060 ± 0.019	0.027 ± 0.014	0.215 ± 0.075	0.145 ± 0.009	1125.3 ± 6.1

All Ar concentrations are in picolitres per gram (pl/g), the calculated ages are in million years, the integrated K_2O and CaO values are in wt.%. The step ages, the plateau ages and the total gas ages are calculated with the Steiger and Jäger (1977) decay constant and age monitor calibrations by Renne et al. (1998). b.d. = below detection limit. Steps used for the calculation of the plateau ages are marked by asterisks.

different compositions do not degas in well-separated breakdown intervals.

The isotopic composition of the released Ar is listed in Table 2 and shown graphically in Fig. 3 in terms of age spectra. The step ages in Table 2 were calculated with the decay constant of Steiger and Jäger (1977) and age monitor calibrations of Renne et al. (1998). The young ages of the first few heating steps not shown in the age spectra (Fig. 3) are the result of gas release from minor alteration products that contribute only a few percent to the total ^{39}Ar. The gas-rich steps have more uniform step ages, mostly in the range 1145–1155 Ma. A statistical analysis of step ages often gives an acceptable low dispersion with MSWD values ranging between 2.0 and 5.4. The steps used to calculate the weighted average age are marked by asterisks in Table 2.

Some of the age spectra show well-defined plateaus, others do not. The weighted average ages of those samples with a plateau scatter around 1150 Ma. The age spectrum of the naujaite (GM1370) is problematic because of the poorly developed plateau (Fig. 3) and hence no plateau age was calculated. In this sample, the Ca content of the amphiboles measured with the microprobe is about twice as high as that calculated from the Ar-isotope analyses (Table 3). A discrepancy of the Ca content is also found in sample GM1303, the alkali granite. The $^{37}Ar/^{39}Ar$ ratios vary by a factor of 2 at most during stepwise heating of the samples (Table 2). This indicates that the analysed amphiboles were not severely contaminated by inclusions capable of distorting the Ca/K ratios. During the irradiation of the samples in the nuclear reactor, ^{37}Ar is produced from ^{40}Ca. If the discrepancy were a result of Ca rich mineral inclusions, the $^{37}Ar/^{39}Ar$ ratios would not be as constant as they are because of the different degassing behaviour of the different minerals. The work on fluid inclusions in the alkali granite by Konnerup-Madsen and Rose-Hansen (1984) showed that, in contrast to the agpaitic rocks, the alkali granite contains mainly aqueous inclusions with highly variable salinities ranging from almost zero to more than 60% NaCl-eq. The chemical composition of the entrapped fluid is not known exactly but components other than NaCl are indicated by the occasional occurrence of sylvite and other minerals as daughter crystals in the inclusions (Konnerup-Madsen and Rose-Hansen, 1984). The composition of the fluid inclusions explains the one order of magnitude higher Cl/K of sample GM1303 (calculated from the Ar isotopes) and may be the reason for the difference in the Ca content derived from the microprobe and the Ar isotopes, respectively.

The slightly different $^{40}Ar/^{39}Ar$ step ages of the two kakortokite varieties (GM1335, GM1337) are possibly due to excess Ar in sample GM1335. The samples originate from different layers of the strongly layered sequence. The red variety (GM1335) comes from a higher level (layer +10, following the numeration of Bohse et al., 1971) than the black one (GM1337, layer +5). Hence, the latter must have formed later when the residual melt was more evolved. With further fractionation the magma became richer in incompatible elements. Villa (1983) showed that cumulates incorporate incompatible elements from the magma including excess Ar. Additionally, the amphiboles in the black variety are euhedral and, hence, an early magmatic phase whereas the amphiboles in the red variety occur interstitially. Therefore, the sample from a higher stratigraphic level could contain higher amounts of incompatible elements including excess Ar and display an older age. The well-developed plateau of sample GM1335 does not argue against excess Ar (von Blanckenburg and Villa, 1988). The naujaite, the corresponding flotation cumulate on the roof of the magma chamber, exhibits an apparent age that is still older than that of the red kakortokite. In this rock, the amphiboles occur interstitially, similar to the red kakortokite. Additionally, no plateau is developed in the age

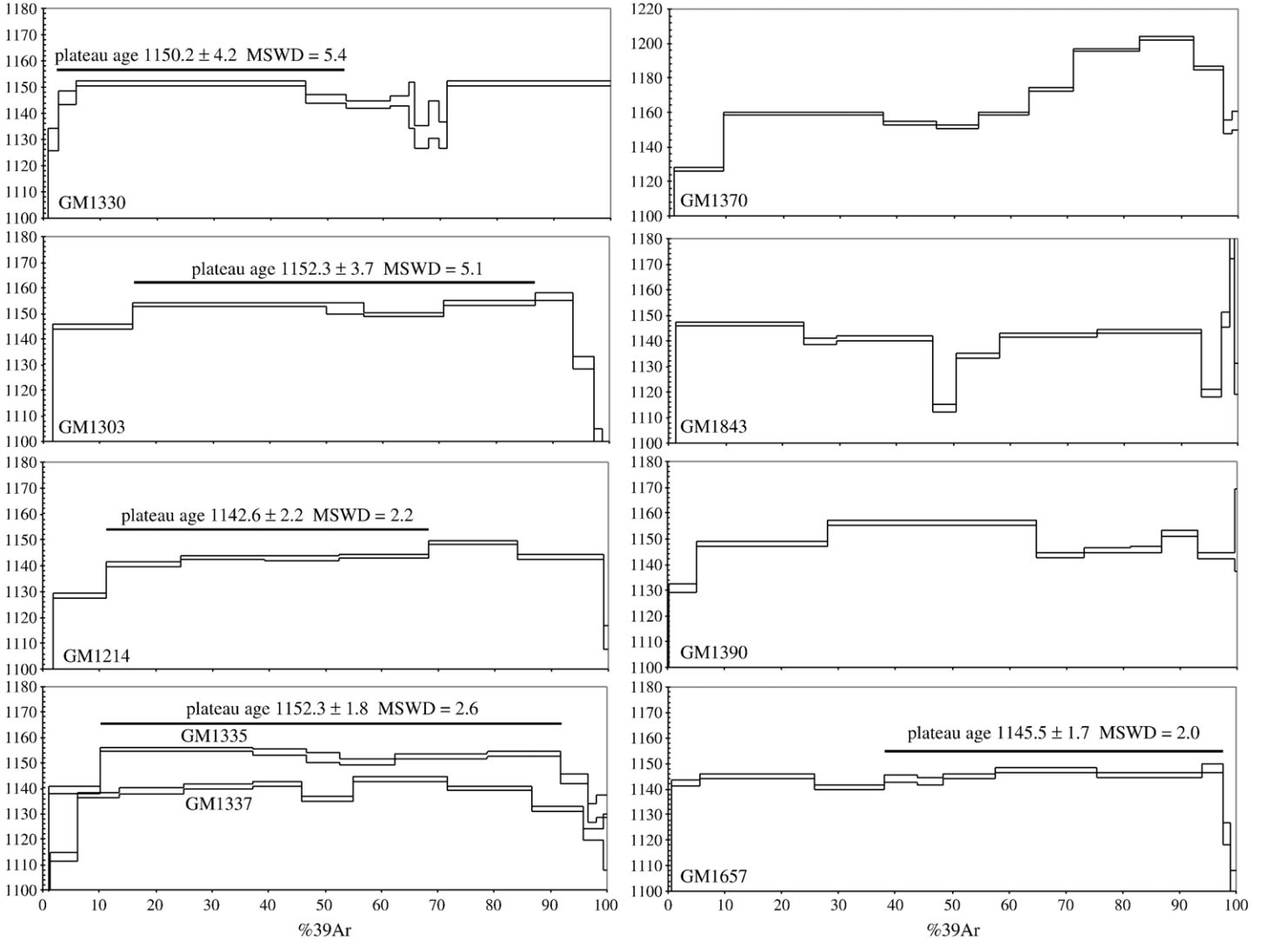

Fig. 3. Age spectra from $^{40}Ar/^{39}Ar$ stepwise heating experiments with the calculated plateau ages. Note the different ages of the two kakortokite samples and the different age scale of sample GM1370. All ages are calculated using the Steiger and Jäger (1977) values for the ^{40}K decay constant and the age monitor calibration by Renne et al. (1998).

Table 3
Comparison of Ca and K contents of the amphiboles measured by the microprobe with those calculated from the released Ar

Sample	GM1330	GM1303	GM1214	GM1370	GM1335	GM1337	GM1390	GM1657	GM1843
Rock type	Augite syenite	Alkali granite	Sodalite foyaite	Naujaite	Kakortokite (red)	Kakortokite (black)	Agpaitic pegmatite	Agpaitic pegmatite	Lujavrite
wt.% microprobe analyses									
CaO	10.89	0.35	2.11	1.47	1.19	1.91	0.31	1.45	0.16
K_2O	1.58	1.40	1.82	2.26	2.13	1.83	2.68	1.71	3.13
CaO/K_2O	6.87	0.25	1.16	0.65	0.56	1.04	0.12	0.85	0.05
Calculated from the Ar-isotopes									
CaO	9.61	1.06	2.60	2.61	1.43	1.56	0.29	1.30	0.16
K_2O	1.59	1.51	1.87	2.09	1.69	1.92	2.85	1.92	2.50
CaO/K_2O	6.04	0.70	1.39	1.25	0.85	0.81	0.10	0.68	0.06

Except samples GM1390, GM1335 and GM1657, the analyses are already published in Marks et al. (2004). The CaO and K_2O values derived from the microprobe are mean values to ensure comparableness with the values calculated from the released Ar.

spectrum of this sample. Konnerup-Madsen et al. (1981) showed that fluid inclusions in amphiboles from the naujaite do contain small quantities of Ar. We therefore cannot rule out fluid inclusions as carriers of excess Ar, which could have decrepitated during step-wise heating between 785 and 980 °C. Isochron treatment of the stepheating data is often used to diagnose the presence of excess Ar, in so far as the intercept on the axis representing trapped Ar may have a different value from atmospheric Ar. However, it is important to point out that the regression must be made only on isochronous reservoirs; from the Ca/Cl/K signature (cf. Villa, 2001) it is straightforward to exclude extraneous phases and restrict the calculation to steps having isochemical Ca/K and Cl/K ratios. If this is done, it can be seen that none of our samples defines an "isochemical isochron" with a trapped Ar significantly different from atmospheric Ar.

5.2. U–Pb radiometric age

Four fractions of baddeleyite from samples GM1857 and GM1858 each consisting of four single grains were chosen for dating with the U–Pb method. The results are shown in Table 4 and in a concordia diagram (Fig. 4). Two fractions are concordant and the other two slightly discordant, whereas one lies above the concordia. This is possibly due to loss of U during the analysis of that particular sample. Another explanation is meteoric leaching of U under oxidising conditions indicated by the lower intercept of the discordia at zero, within uncertainty. Excess ^{207}Pb caused by initial ^{231}Pa in the melt as found by Anczkiewicz et al. (2001) in zircons from an alkali granite dyke would move the point only to higher $^{207}Pb/^{235}U$ ratios but not to both, higher $^{207}Pb/^{235}U$ and higher $^{206}Pb/^{238}U$ values, as observed in the inverse discordant sample. The four data points together define a discordia that intersects the concordia exactly where the two concordant data points lie. An intercept age of 1160 ± 5 Ma with a MSWD of 0.55 was calculated.

6. Discussion

Peralkaline to agpaitic rocks have an unusually long crystallisation interval between 950 and ~450 °C since

Table 4
Isotopic data for baddeleyite from the augite syenite

Sample	Weight[a] (μg)	$^{206}Pb/^{204}Pb$[b]	U[a] ppm	Pb[a] ppm	Th/U[c]	Isotopic ratios[d]						Calculated ages (Ma)		
						$^{206}Pb/^{238}Pb$	±	$^{207}Pb/^{235}Pb$	±	$^{207}Pb/^{206}Pb$	±	$^{206}Pb/^{238}Pb$	$^{206}Pb/^{235}Pb$	$^{207}Pb/^{206}Pb$
GM1858A	8	16.9	106	19	1.7	0.1956	20	2.116	22	0.078437	68	1151.9	1154.0	1158.0
GM1858B	10	18.7	37	7	5.0	0.2108	22	2.287	24	0.078691	176	1232.9	1208.2	1164.4
GM1857C	15	16.9	986	180	0.19	0.1962	20	2.123	22	0.078492	40	1154.8	1156.4	1159.3
GM1857D	10	16.9	374	66	0.50	0.1881	29	2.035	31	0.078487	95	1111.0	1127.4	1159.2

[a] Weight and concentration error better than 20%.
[b] Measured ratio corrected for mass discrimination and spike contribution.
[c] Th/U model ratio calculated from $^{208}Pb/^{206}Pb$ ratio and age of the sample.
[d] Corrected for blank Pb, U, and initial common Pb based on the Stacey and Kramers (1975) model, errors are 2σ.

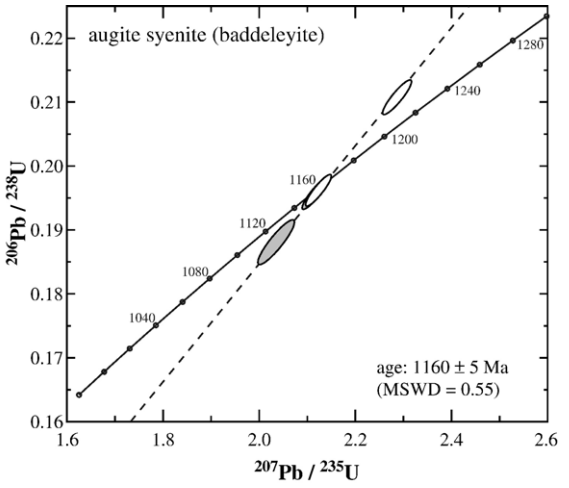

Fig. 4. Concordia diagram of samples GM1857 (grey) and GM1858 (white) from the augite syenite.

the volatiles are retained in the melt during most of the crystallisation history (Boily and Williams-Jones, 1994; Markl et al., 2001a). The solidus of the agpaitic melt lies at temperatures well below the closure temperature of the amphiboles. While the re-evaluated closure temperature of hornblende sensu stricto is about 600 °C for a cooling rate >10 °C/Ma (Villa, 1998), it is necessary to take into account the ionic porosity (Dahl, 1997) of the alkali amphiboles to estimate their Ar retentivity. This results in a lower closure temperature of approximately 500 to 550 °C. Hence, the geochronological watch started to tick while the amphiboles in the agpaitic rocks were still surrounded by melt. Consequently, the $^{40}Ar/^{39}Ar$ ages of the agpaitic rocks clearly reflect magmatic processes.

6.1. Rb–Sr ages

The Rb–Sr age for the kakortokite by Waight et al. (2002) recalculated with the ^{87}Rb decay constant given by Begemann et al. (2001) is 1175 Ma and, hence, not in agreement with the U–Pb data. Following the field relationships of the Ilímaussaq rocks, the agpaites including the kakortokites developed from the youngest magma batch. The Rb–Sr age by Waight et al. (2002) is based on a two point isochron using eudialyte and alkali feldspar. The whole rock is not included but they assumed the Rb/Sr ratio of the whole rock to be zero. Bailey et al. (2001) showed that the kakortokites contain up to 540 ppm Rb. Consequently, the whole rock point would not be zero as assumed by Waight et al. (2002). Parsons et al. (1988) demonstrated that alkali feldspars in plutons are likely to have structural damages in terms of micropores. This also may have affected the Rb–Sr system. We therefore conclude that the recalculated Rb–Sr age of Waight et al. (2002) is not reliable.

Blaxland et al. (1976) presented Rb–Sr data, from which they calculated a whole rock isochron of 1168 ± 21 Ma. From the data in their Tables 1 and 2 we recalculated the isochrons, both using the ^{87}Rb decay constant used by them (1.39×10^{-11} a^{-1}) and a revised one of 1.402×10^{-11} a^{-1} as summarised by Begemann et al. (2001). The former indeed gives 1168 ± 24 Ma, but the MSWD is 53 rather than 3.6; this very high scatter suggests that the whole-rock system may not represent a suitable chronometer. In any case, the apparent age formally calculated with the revised ^{87}Rb decay constant is 1158 ± 24 Ma which agrees with the U–Pb baddeleyite age.

6.2. ^{40}K decay constant

The decay constant of ^{40}K currently used in geochronology is 5.543×10^{-10} a^{-1} and was recommended by the IUGS Subcommission on Geochronology (Steiger and Jäger, 1977). In recent times it has been suggested that the uncertainties in the radioactive decay constants can be a source of systematic error (Begemann et al., 2001). The ^{40}K decay constant is still a matter of debate and several workers re-examined the values (Min et al., 2000; Kwon et al., 2002; Villa and Renne, 2005). A peculiarity of the K–Ar system, which further complicates the attainment of reliable age estimates, is the difficulty of performing a precise and accurate determination of absolute volumes of radiogenic Ar, and the consequent widespread use of "age monitors" to indirectly calibrate the ages of unknown samples. The age monitors themselves have been dated with finite precision and accuracy. The review paper by Renne et al. (1998) proposes an intercalibration of several age monitors, including MMhb1 used in the present study, relative to each other. For historical reasons, the Fish Canyon Tuff sanidine monitor (FCT) is used as a pivot for the other monitors. The FCT age was estimated at 28.02 ± 0.16 Ma by Renne et al. (1998).

Our samples are germane to the problem of assessing the various estimates of the ^{40}K decay constant from the literature. For the discussion's sake, we can assume either (i) that most samples do not contain excess Ar, or (ii) that most of them do, neglecting, for the time being, our argument in the previous section. In case (i), the calculation with the constant of Steiger and Jäger (1977) results in ages around 1145 Ma, significantly younger than the U–Pb ages of 1160 Ma (Fig. 5a). To explain this large age difference, one

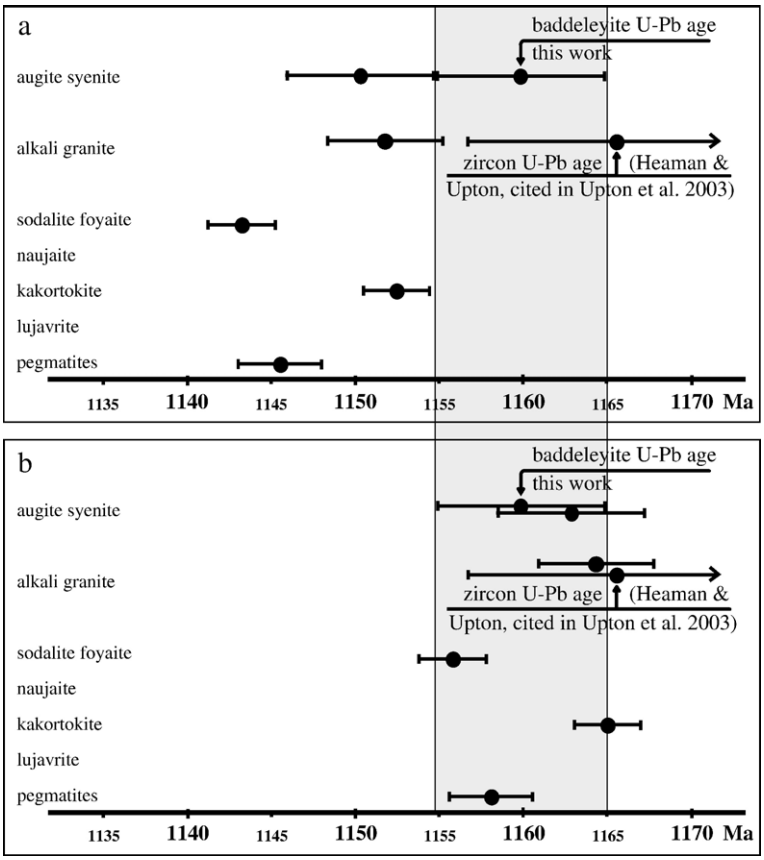

Fig. 5. Diagram comparing the amphibole $^{40}Ar/^{39}Ar$ ages (unlabeled points), the baddeleyite U/Pb age and ages published elsewhere. The grey box indicates the proposed age of intrusion, given by our U–Pb age. (a) $^{40}Ar/^{39}Ar$ ages calculated using the ^{40}K decay constant of Steiger and Jäger (1977) and age monitor calibration by Renne et al. (1998). (b) $^{40}Ar/^{39}Ar$ ages calculated using revised values. Note the conformity of the different dating methods.

has to postulate either an intrusion history with a gap of 15 Ma between the younger agpaitic series and the older augite syenite and alkali granite, or a prolonged history of isotopically open behaviour. In the first case, the intrusion of the agpaites has to reset the amphiboles of the earlier rocks completely. Additionally, the deep-seated magma chamber is required to be stable over 15 Ma. As pointed out by Marks et al. (2004), all Ilímaussaq rocks have a single source. Fractionation in a deep-seated magma chamber from the augite syenite to the agpaitic rocks would have to last those 15 Ma, which is unreasonable according to work by several authors who have shown that differentiation is a much faster process (e.g. Christensen and DePaolo, 1993; Reid et al., 1997; Hawkesworth et al., 2000; Reagan et al., 2003). The possibility that the amphiboles record delayed "cooling ages" can, as explained in the Appendix, also be ruled out. All independent arguments request that the amphiboles be 1160 Ma old. Based on this geological, petrological and isotopical argumentation, we conclude that using the Steiger and Jäger (1977) ^{40}K decay constant and the FCT age of 28.02 Ma results in inaccurate $^{40}Ar/^{39}Ar$ ages. In case (ii), we should consider the age of the youngest sample, GM1337, as the least affected by excess Ar. The "true age" of the amphiboles would thus become 1138 Ma. This requires a much larger correction to the decay constant and/or the FCT age than case (i). Seeing as in a preceding paragraph we argued that excess Ar was unlikely to have affected more than a few outliers, we believe that case (i) requiring the smaller correction is the more conservative and realistic one.

In order to reduce the 15 Ma age gap between the U–Pb and K–Ar systems to zero, one can modify (a) the decay constant, but not the FCT age, (b) modify the FCT age, but not the decay constant, (c) modify both simultaneously. Approach (c) has been followed by Kwon et al. (2002) who proposed a decay constant for ^{40}K of $(5.476 \pm 0.034) \times 10^{-10}$ a^{-1} and an FCT age of 28.27 ± 0.13 Ma. For our amphiboles, these

values produce ages around 1170 Ma under assumption (i). Approach (b) has been followed by Kuiper et al. (2004) who compared cyclostratigraphic ages with interbedded tephras and derived an FCT age of 28.24 ± 0.01 Ma all while keeping the Steiger and Jäger (1977) decay constant. In our case, this results in amphibole ages around 1155 Ma under assumption (i). Finally, approach (a) is not represented in the recent literature. Clearly, our single data-set is not capable of simultaneously solving for three unknowns (FCT age, decay constant, and possible concentration of excess Ar), but still can provide constraints on the magnitude of the changes to either of the former two parameters.

7. Summary and conclusions

Both amphiboles and baddeleyite recorded the intrusion of the Ilímaussaq complex. After their intrusion, the rocks were not affected by any metamorphic overprint. Therefore, we can use these magmatic rocks as a "point-like geological event" sensu Begemann et al. (2001) to provide constraints on the intercalibration of the K–Ar and U–Pb clocks. Comparing the U–Pb ages from the augite syenite (this work) and the alkali granite (Heaman and Upton, cited in Upton et al., 2003) with our apparent ^{40}Ar–^{39}Ar ages on amphiboles strongly suggests that the K–Ar system suffers from a systematic bias when calculated using the Steiger and Jäger (1977) decay constants in conjunction with an FCT monitor age of 28.02 Ma. Furthermore, the recalculated Rb–Sr age of Blaxland et al. (1976) and the Sm–Nd ages by Paslick et al. (1993) and by Marks et al. (2004) give also ages around 1160 Ma even though these ages are loaded with a much larger error. The geology, the petrology, the isotopic composition and the thermal modelling argue for the use of a new ^{40}K decay constant close to that published by Kwon et al. (2002).

The time of formation of the Ilímaussaq complex can be fixed at 1160 ± 5 Ma (Fig. 5). The development of the complex is characterised by a short-lived fractionation history in a deep-seated magma chamber from the parental phonolitic melt to an agpaitic one. From this magma chamber, two early magma batches (augite syenite and alkali granite) and one late batch (agpaitic nepheline syenites) were injected into the upper crust. The last batch underwent further fractionation at the final level of intrusion forming cumulates both on the roof and on the bottom of the upper crustal magma chamber. The time span needed for this fractionation is limited by the Ar results to a maximum of 5 million years, presumably much shorter on the order of 500 to 800 ka as indicated by the thermal modelling and the conformity of the results from all dating methods.

Acknowledgements

Wolfgang Siebel is thanked for his careful U–Pb isotope measurements and his improvement of a former version of the manuscript. Gisela Bartholomae provided invaluable help during mineral separation. Florian Wehland helped with the thermal modelling. Two reviews by James K. Lee and an anonymous referee are gratefully acknowledged. Financial support for this work was funded by the Deutsche Forschungsgemeinschaft (grant Ma-2135/4-2).

This is Contribution to the mineralogy of Ilímaussaq No. 124. **[RLR]**

Appendix A. Cooling model

In order to test independently the validity of our geochronological results, we modelled the thermal evolution of the Ilímaussaq complex after its intrusion.

The geometry of the intrusion (Sørensen, 2001), the physical properties of the intrusives and the host rocks (Forsberg and Rasmussen, 1978) and the intrusion level of 3–4 km (e.g. Larsen and Sørensen, 1987) are well known. Mafic cumulates at depth are indicated by a positive gravity anomaly beneath the complex (Blundell, 1978; Forsberg and Rasmussen, 1978). However, Blundell (1978) related the anomaly to a gabbroic body and interpreted the Narssaq intrusion as its surface expression. Based on field observations, the Narssaq intrusion predates the Ilímaussaq complex. Therefore, the gravity anomaly may not be caused by basal cumulates of the Ilímaussaq magmas.

Several processes influence the cooling history. As pointed out by Furlong et al. (1991), circulation of a fluid phase through the pluton would enhance cooling. However, the Ilímaussaq intrusion can be regarded as a closed system (Marks et al., 2004) even during late stage hydrothermal activity (Markl et al., 2001a). Accordingly, no fluid phase from the surrounding had access to the intrusive body or escaped from it and the heat transport to the host rocks must have been dominated by conduction. Cooling can be enhanced by vaporisation of fluid in the host rocks close to a pluton (Shaw et al., 1977; Delaney, 1984). Another fact that accelerates the cooling especially of shallow intrusions is a high thermal gradient between host rock and magma body. This is expected to be the most important feature with regards to the cooling of the Ilímaussaq complex.

Some assumptions concerning the starting conditions of the model had to be made. The geothermal gradient was assumed to be higher than normal because of the large amount of magma penetrating the crust and forming the alkaline intrusions and the basalts of the Eriksfjord formation in an extensional rift setting. Accordingly, the calculations were carried out with a geothermal gradient of 50°/km. However, tests during modelling showed that this higher geothermal gradient extends the cooling of the pluton below the closure temperature of the amphiboles only in that way that it has no consequence for the interpretation. Another assumption is the way of transporting the heat. As pointed out above, we believe that heat conduction at least close to the pluton is the favourable mechanism. Formation of a convection cell in the host rocks is especially likely in the subaerial to submarine (Poulsen, 1964) and hence fluid-saturated basalts and sandstones of the Eriksfjord formation. It is still not clear, whether the Eriksfjord formation is partly contemporaneous with the Ilímaussaq intrusion or not (Halama et al., 2003; Upton et al., 2003). Based on field observations, the Ilímaussaq rocks clearly intruded the basaltic lava flows, which can be found as xenoliths especially in the upper part of the intrusion. Several dating studies using both isotopes and paleomagnetics were carried out resulting in ages between 1.17 and 1.35 Ga (Paslick et al., 1993; Andersen, 1997; Piper et al., 1999). The youngest age of 1170 ± 30 Ma published by Paslick et al. (1993) from the second of three volcanic groups indicates the possibility that the upper parts of the Eriksfjord basalts are contemporaneous with the Ilímaussaq rocks or even post-date them providing a heat source above the pluton. The effect on the duration of the cooling is, however, minor and can be disregarded. The volumes of the two earlier magma batches, especially that of the alkali granite, are small. They should have cooled down very fast. From field observation it is known that the two earlier rocks were solidified when the agpaites intruded. Therefore, we decided to create a simple model without magma rejuvenation.

For thermal modelling, we used the latest version of the freely available HEAT 3D software. A former version of the software is described in Wohletz and Heiken (1992). Models were calculated using the 3D mode of the HEAT 3D software with different starting conditions considering the problems mentioned above. The results are surprisingly uniform. The intrusion cooled to 500 °C within at most 800 ka (Fig. A2).

Appendix B. Supplementary data

Supplementary data associated with this article can be found, in the online version, at doi:10.1016/j.chemgeo.2005.10.004.

References

Anczkiewicz, R., Oberli, F., Burg, J.P., Villa, I.M., Günther, D., Meier, M., 2001. Timing of normal faulting along the Indus Suture in Pakistan Himalaya and a case of major $^{231}Pa/^{235}U$ initial disequilibrium in zircon. Earth Planet. Sci. Lett. 191, 101–114.

Andersen, T., 1997. Age and petrogenesis of the Qassiarsuk carbonatite–alkaline silicate volcanic complex in the Gardar rift, South Greenland. Min. Mag. 61, 499–513.

Arzamastsev, A.A., Belyatsky, B.V., Arzamastseva, L.V., 2000. Agpaitic magmatism in the northeastern Baltic Shield: a study of the Niva intrusion Kola Peninsula, Russia. Lithos 51, 27–46.

Bailey, J.C., Gwozdz, R., Rose-Hansen, J., Sørensen, H., 2001. Geochemical overview of the Ilímaussaq complex, South Greenland. In: Sørensen, H. (Ed.), The Ilímaussaq alkaline complex, South Greenland: status of mineralogical research with new results, Geol. Greenl. Surv. Bull., vol. 190, pp. 35–54.

Begemann, F., Ludwig, K.R., Lugmair, G.W., Min, K., Nyquist, L.E., Patchett, P.J., et al., 2001. Call for an improved set of decay constants for geochronological use. Geochim. Cosmochim. Acta 65, 111–121.

Blaxland, A.B., van Breeman, O., Steenfelt, A., 1976. Age and origin of agpaitic magmatism at Ilimaussaq, South Greenland: Rb–Sr study. Lithos 9, 31–38.

Blundell, D.J., 1978. A gravity survey across the Gardar Igneous Province, SW Greenland. J. Geol. Soc. London 135, 545–554.

Bohse, H., Brooks, C.K., Kunzendorf, H., 1971. Field observations on the kakortikites of the Ilímaussaq intrusion, South Greenland, including mapping and analyses by portable X-ray fluorescence equipment for zirconium and niobium. Rapp. Grønl. Geol. Unders. 38, 43.

Boily, M., Williams-Jones, A.E., 1994. The role of magmatic and hydrothermal processes in the chemical evolution of the Strange Lake plutonic complex, Quebec–Labrador. Contrib. Mineral. Petrol. 118, 33–47.

Bourdon, B., Zindler, A., Wörner, G., 1994. Evolution of the Laacher See magma chamber: evidence from SIMS and TIMS measurements of U–Th disequilibria in minerals and glasses. Earth Planet. Sci. Lett. 126, 75–90.

Chen, F., Hegner, E., Todt, W., 2000. Zircon ages and Nd isotopic and chemical compositions of orthogneisses from the Black forest, Germany: evidence for a Cambrian magmatic arc. Int. J. Earth Sci. 88, 791–802.

Christensen, J.N., DePaolo, D.J., 1993. Time scales of large volume silicic magma systems; Sr isotopic systematics of phenocrysts and glass from the Bishop Tuff, Long Valley, California. Contrib. Mineral. Petrol. 113, 100–114.

Dahl, P.S., 1997. A crystal-chemical basis for Pb retention and fission-track annealing systematics in U-bearing minerals, with implications for geochronology. Earth Planet. Sci. Lett. 150, 270–299.

Delaney, P.T., 1984. Heating of a fully saturated Darcian half-space: pressure generation, fluid expulsion and phase change. Int. J. Heat Mass Transfer 27, 1327–1335.

Ferguson, J., 1964. Geology of the Ilimaussaq alkaline intrusion, South Greenland. Bull. Grønl. Geol. Unders. 39, 82.

Forsberg, R., Rasmussen, K.L., 1978. Gravity and rock densities in the Ilímaussaq area, South Greenland. Rapp. Grønl. Geol. Unders. 90, 81–84.

Furlong, K.P., Hnason, R.B., Bowers, J.R., 1991. Modeling thermal regimes. In contact metamorphism. In: Kerrick, D.M.Rev. Mineral, vol. 26, pp. 437–497.

Halama, R., Wenzel, T., Upton, B.G.J., Siebel, W., Markl, G., 2003. A geochemical and Sr–Nd–O isotopic study of the Proterozoic Eriksfjord Basalts, Gardar Province, South Greenland: Reconstruction of an OIB signature in crustally contaminated rift-related basalts. Min. Mag. 67, 831–853.

Harris, C., Marsh, J.S., Milner, S.C., 1999. Petrology of the alkaline core of the Messum igneous complex, Namibia: evidence for the progressively decreasing effect of crustal contamination. J. Petrol. 40, 1377–1397.

Hawkesworth, C.J., Blake, S., Evans, P., Hughes, R., Macdonald, R., Thomas, L.E., et al., 2000. Time scales of crystal fractionation in magma chamber—integrating physical, isotopic and geochemical perspectives. J. Petrol. 41, 991–1006.

Heaman, L.M., Machado, N., 1992. Timing and origin of midcontinent rift alkaline magmatism, North America: evidence from the Coldwell Complex. Contrib. Mineral. Petrol. 110, 289–303.

Konnerup-Madsen, J., Rose-Hansen, J., 1984. Composition and significance of fluid inclusions in the Ilímaussaq peralkaline granite, South Greenland. Bull. Mineral. 107, 317–326.

Konnerup-Madsen, J., Rose-Hansen, J., Larsen, E., 1981. Hydrocarbon gases associated with alkaline igneous activity: evidence from compositions of fluid inclusions. Rapp. Grønl. Geol. Unders. 103, 99–108.

Kramm, U., Kogarko, L.N., Kononova, V.A., Vartiainen, H., 1993. The Kola Alkaline Province of the CIS and Finland: precise Rb–Sr age define 380–360 Ma age range for all magmatism. Lithos 30, 33–44.

Kramm, U., Kogarko, L.N., 1994. Nd and Sr isotope signatures of the Khibina and Lovozero agpaitic centres, Kola Alkaline Province, Russia. Lithos 32, 225–242.

Kuiper, K., Hilgen, F.J., Krijgsman, W., Wijbrans, J., 2004. An astronomically dated standard in $^{40}Ar/^{39}Ar$ geochronology? Abstract, 32nd Internat. Geol. Congress, Firenze, 812.

Kwon, J., Min, K., Bickel, P., Renne, P.R., 2002. Statistical methods for jointly estimating decay constant of ^{40}K and age of a dating standard. Math. Geol. 34, 457–474.

Larsen, L.M., 1976. Clinopyroxenes and coexisting mafic minerals from the alkaline Ilimaussaq intrusion, South Greenland. J. Petrol. 17, 258–290.

Larsen, L.M., 1977. Aenigmatites from the Ilimaussaq intrusion, South Greenland: chemistry and petrological implications. Lithos 10, 257–270.

Larsen, L.M., 1981. Chemistry of feldspars in the Ilímaussaq augite syenite with additional data on some other minerals. Rapp. Grønl. Geol. Unders. 103, 31–37.

Larsen, L.M., Sørensen, H., 1987. The Ilímaussaq intrusion — progressive crystallisation and formation of layering in an agpaitic magma. In: Fitton, J.G., Upton, B.G.J. (Eds.), Alkaline Igneous Rocks, Geol. Soc. Sp. Publ. London, vol. 30, pp. 473–488.

Lee, J.K.W., 1993. The argon release mechanisms of hornblende in vacuo. Chem. Geol. 106, 133–170.

Ludwig, K.R., 1988. PBDAT for MS-DOS: a computer program for IBM-PC compatibles for processing raw Pb–U–Th isotope data. U.S. Geological Survey Open-File Report, pp. 88–0542.

Ludwig, K.R., 2003. Isoplot 3.00—a geochronological toolkit for Microsoft Excel: Berkeley Geochronology Center. Spec Publ., vol. 4.

Markl, G., 2001. Stability of Na–Be minerals in late-magmatic fluids of the Ilímaussaq alkaline complex, South Greenland. In: Sørensen, H. (Ed.), The Ilímaussaq alkaline complex, South Greenland: status of mineralogical research with new results, Geol. Greenl. Surv. Bull., vol. 190, pp. 145–158.

Markl, G., Marks, M., Schwinn, G., Sommer, H., 2001a. Phase equilibrium constraints on intensive crystallization parameters of the Ilimaussaq Complex, South Greenland. J. Petrol. 42, 2231–2258.

Markl, G., Marks, M., Wirth, R., 2001b. The influence of T, $aSiO_2$, fO_2 on exsolution textures in Fe–Mg olivine: an example from augite syenite of the Ilimaussaq Intrusion, South Greenland. Am. Mineral. 86, 36–46.

Marks, M., Markl, G., 2001. Fractionation and assimilation processes in the alkaline augite syenite unit of the Ilimaussaq Intrusion, South Greenland, as deduced from phase equilibria. J. Petrol. 42, 1947–1969.

Marks, M., Vennemann, T., Siebel, W., Markl, G., 2004. Nd-, O-, and H-isotopic evidence for complex, closed-system fluid evolution of the peralkaline Ilímaussaq Intrusion, South Greenland. Geochim. Cosmochim. Acta 68, 3379–3395.

Min, K., Mundil, R., Renne, P.R., Ludwig, K.R., 2000. A test for systematic errors in $^{40}Ar/^{39}Ar$ geochronology through comparision with U/Pb analysis of a 1.1-Ga rhyolite. Geochim. Cosmochim. Acta 64, 73–98.

Mingram, B., Trumbull, R.B., Littman, S., Gerstenberger, H., 2000. A petrogenetic study of anorogenic felsic magmatism in the Cretaceous Paresis ring complex, Namibia, evidence for mixing of crust and mantle-derived components. Lithos 54, 1–22.

Nielsen, B.L., Steenfelt, A., 1979. Intrusive events at Kvanefjeld in the Ilímaussaq igneous Complex. Bull. Geol. Soc. Denmark 27, 143–155.

Parsons, I., Rex, D.C., Guise, P., Halliday, A.N., 1988. Argon-loss by alkali feldspars. Geochim. Cosmochim. Acta 52, 1097–1112.

Paslick, C.R., Halliday, A.N., Davies, G.R., Mezger, K., Upton, B.G.J., 1993. Timing of proterozoic magmatism in the Gardar Province, Southern Greenland. Bull. Geol. Soc. America 105, 272–278.

Piper, J.D.A., Thomas, D.N., Share, S., Zhang Qi Rui, 1999. The palaeomagnetism of (Mesoproterozoic) Eriksfjord Group red beds, South Greenland: multi-phase remagnetization during the Gardar and Grenville episodes. Geophys. J. Int. 136, 739–756.

Poulsen, V., 1964. The sandstones of the Precambrian Eriksfjord Formation in South Greenland. Rapp. Grønl. Geol. Unders. 2, 16.

Reagan, M.K., Sims, K.W.W., Erich, J., Thomas, R.B., Cheng, H., Edwards, R.L., et al., 2003. Time-scales of differentiation from mafic parents to rhyolite in North American Continental Arcs. J. Petrol. 44, 1703–1726.

Reid, M.R., Coath, C.D., Harrison, T.M., McKeegan, K.D., 1997. Prolonged residence times for the youngest rhyolites associated with Long Valley Caldera; $^{230}Th–^{238}U$ ion microprobe dating of young zircons. Earth Planet. Sci. Lett. 150, 27–39.

Renne, P.R., Swisher, C.C., Deino, A.L., Karner, D.B., Owens, T.L., DePaolo, D.J., 1998. Intercalibration of standards, absolute ages and uncertainties in $^{40}Ar/^{39}Ar$ dating. Chem. Geol. 145, 117–152.

Rogers, N.W., Evans, P.J., Blake, S., Scott, S.C., Hawkesworth, C.J., 2004. Rates and timescales of fractional crystallisation from $^{238}U–^{230}Th–^{226}Ra$ disequilibria in trachyte lavas from Longonot volcano, Kenya. J. Petrol. 45, 1747–1776.

Rose-Hansen, J., Sørensen, H., and Watt, W.S., 2001. Inventory of the literature on the Ilímaussaq alkaline complex, South Greenland. Dan. Grønl. Geol. Unders. Rapp. 2000/57, 38 pp. +CD-ROM.

Schmitt, A.K., Emmermann, R., Trumbull, R.B., Bühn, B., Henjes-Kunst, F., 2000. Petrogenesis and $^{40}Ar/^{39}Ar$ geochronology of the Brandberg Complex, Namibia: evidence for a major mantle contribution in metaluminous and peralkaline granites. J. Petrol. 41, 1207–1239.

Shaw, H.R., Hamilton, M.S., Peck, O.L., 1977. Numerical analysis of lava lake cooling model. I. Description of model. Am. J. Sci. 277, 384–414.

Sørensen, H., 1966. On the magmatic evolution of the alkaline igneous province of South Greenland. Rapp. Grønl. Geol. Unders. 7, 1–19.

Sørensen, H., 2001. Brief introduction to the geology of the Ilímaussaq alkaline complex, South Greenland, and its exploration history. In: Sørensen, H. (Ed.), The Ilímaussaq alkaline complex, South Greenland: status of mineralogical research with new results, Geol. Greenl. Surv. Bull., vol. 190, pp. 7–24.

Sørensen, H., Larsen, L.M., 1987. The Ilimaussaq Intrusion; progressive crystallization and formation of layering in an agpaitic magma. In: Fitton, J.G., Upton, B.G.J. (Eds.), Alkaline igneous rocks, Geol. Soc. Spec. Publ., vol. 30, pp. 473–488.

Stacey, J.S., Kramers, J.D., 1975. Approximation of terrestrial lead isotope evolution by a two stage model. Earth Planet. Sci. Lett. 127, 30–45.

Steiger, R.H., Jäger, E., 1977. Subcommision on Geochronology: convention on the use of decay constants in geo- and cosmochronology. Earth Planet. Sci. Lett. 36, 359–362.

Stevenson, R., Upton, B.G.J., Steenfelt, A., 1997. Crust–mantle interaction in the evolution of the Ilímaussaq Complex, South Greenland: Nd isotopic studies. Lithos 40, 189–202.

Upton, B.G.J., Emeleus, C.H., Heaman, L.M., Goodenough, K.M., Finch, A.A., 2003. Magmatism of the mid-Proterozoic Gardar Province, South Greenland: chronology, petrogenesis and geological setting. Lithos 68, 43–65.

Ussing, N.V., 1912. Geology of the country around Julianehaab, Greenland. Medd. Grønl. 38, 426.

Villa, I.M., 1983. $^{40}Ar/^{39}Ar$ chronology of the Adamello gabbros, Southern Alps. Mem. Soc. Geol. Ital. 26 (1), 309–318.

Villa, I.M., 1998. Isotopic closure. Terra Nova 10, 42–47.

Villa, I.M., 2001. Radiogenic isotopes in fluid inclusions. Lithos 55, 115–124.

Villa, I.M., Renne, P.R., 2005. Decay constants in geochronology. Episodes 28, 50–51.

Villa, I.M., Hermann, J., Müntener, O., Trommelsdorf, V., 2000. ^{39}Ar–^{40}Ar dating of multiply zoned amphibole generations (Malenco, Italian Alps). Contrib. Mineral. Petrol. 140, 363–381.

von Blanckenburg, F., Villa, I.M., 1988. Argon retentivity and argon excess in amphiboles from the graben schists of the Western Tauern Window, Eastern Alps. Contrib. Mineral. Petrol. 100, 1–11.

Waight, T., Baker, J., Willigers, B., 2002. Rb isotope dilution analyses by MC-ICPMS using Zr to correct for mass fractionation: towards improved Rb–Sr geochronology? Chem. Geol. 186, 99–116.

Wartho, J.A., Dodson, M.H., Rex, D.C., Guise, P.G., 1991. Mechanisms of Ar release from Himalayan metamorphic hornblende. Am. Mineral. 76, 1446–1448.

Widom, E., Schmincke, H.U., Gill, J.B., 1992. Process and timescales in the evolution of a chemically zoned trachyte: Fogo A, Sao Miguel, Azores. Contrib. Mineral. Petrol. 111, 311–328.

Wohletz, K., Heiken, G., 1992. Volcanology and Geothermal Energy. University of California Press, Berkeley p. 432.